# First light adaptive optics systems and components for the Thirty Meter Telescope

Brent Ellerbroek[1a], Sean Adkins[b], David Andersen[c], Jenny Atwood[c], Steve Browne[d], Corinne Boyer[a], Peter Byrnes[c], Kris Caputa[c,] Rodolphe Conan[e], Raphael Cousty[f], Daren Erikson[c], Joeleff Fitzsimmons[c,] Frederick Gamache[g], Luc Gilles[a], Glen Herriot[c], Paul Hickson[h], Olivier Lardier[e], Pierre Morin[f], John Pazder[c,] Thomas Pfrommer[h], David Quinn[g], Vladimir Reshetov[c], Scott Roberts[c] Jean-Christophe Sinquin[f], Matthias Schoeck[c], Malcolm Smith[c], Glenn Tyler[d], Jeff Vaughn[d], Jean-Pierre Veran[c], Curt Vogel[i], Lianqi Wang[a], and Ivan Wevers[c]

[a]TMT Observatory Corporation, 2632 E. Washington Blvd, Pasadena, CA USA 91107;
[b]W. M. Keck Observatory, 65-1120 Mamalahoa Highway, Kamuela, HI USA 96743;
[c]Herzberg Institute of Astrophysics, 5071 W. Saanich Road, Victoria, BC Canada V9E 2E7;
[d]the Optical Sciences Company, 1341 S. Sunkist St., Anaheim, CA USA 92806;
[e]University of Victoria, PO Box 3055 STN CSC, Victoria, BC Canada V8W 3P6;
[f]CILAS, 8 Avenue Buffon - ZI La Source, Orleans, France 45100
[g]Lyrtech, 2800 Louis-Lumiere St., Quebec City, Quebec Canada G1P 0A4 ;
[h]University of British Columbia, 6224 Agricultural Road, Vancouver, BC Canada V6T 1Z1;
[i]Department of Mathematical Sciences , Montana State University ,Bozeman, MT USA 59717-2400

## ABSTRACT

Adaptive optics (AO) is essential for many elements of the science case for the Thirty Meter Telescope (TMT). The initial requirements for the observatory's facility AO system include diffraction-limited performance in the near IR, with 50 per cent sky coverage at the galactic pole. Point spread function uniformity and stability over a 30 arc sec field-of-view are also required for precision photometry and astrometry. These capabilities will be achieved via an order 60x60 multi-conjugate AO system (NFIRAOS) with two deformable mirrors, six laser guide star wavefront sensors, and three low-order, IR, natural guide star wavefront sensors within each client instrument. The associated laser guide star facility (LGSF) will employ 150W of laser power at a wavelength of 589 nm to generate the six laser guide stars.

We provide an update on the progress in designing, modeling, and validating these systems and their components over the last two years. This includes work on the layouts and detailed designs of NFIRAOS and the LGSF; fabrication and test of a full-scale prototype tip/tilt stage (TTS); Conceptual Designs Studies for the real time controller (RTC) hardware and algorithms; fabrication and test of the detectors for the laser- and natural-guide star wavefront sensors; AO system modeling and performance optimization; lab tests of wavefront sensing algorithms for use with elongated laser guide stars; and high resolution LIDAR measurements of the mesospheric sodium layer. Further details may be found in specific papers on each of these topics.

**Keywords:** Extremely Large Telescopes, Adaptive Optics

## 1. INTRODUCTION

The TMT Project[1] is proceeding towards the construction of a 30-meter optical/infra-red telescope for research in astronomy. The ongoing development of subsystem-level requirements, designs, analyses, and prototype test results is progressing, as is described in other papers presented at this symposium[2-10].

Adaptive optics (AO) remains essential for many if not most TMT science cases[11]. The fundamental requirements for the early light AO systems have remained largely the same over the last two years. However, important changes have occurred in the design of the Narrow Field Infra Red AO System (NIRAOS) to eliminate the time-varying image distortion that was originally overlooked. The concept for the Laser Guide Star Facility (LGSF) has also been updated

to capitalize upon recent progress in guide star laser technology. Additional progress has also occurred for other AO component technologies, including wave front correctors, visible and near infrared wave front sensor (WFS) detectors, and the real-time controller (RTC) electronics and algorithms. Finally, work continues to assess and optimize the overall performance of the full system through a combination of modeling, lab experiments, and field measurements. Further information on these topics is given below, and in other papers from this meeting[12-22] and prior publications[23-27].

# 2. AO REQUIREMENTS AND THE DERIVED SYSTEM ARCHITECTURE

## 2.1 Top-level and derived requirements

The top-level requirements for the TMT early light AO are listed in our Observatory Requirements Document (ORD)[28], and the traceability from these requirements to the AO system architecture has been described earlier[29-30]. The central points are reviewed in Table 1 below. The derived requirement for negligible time-varying image distortion is *highlighted*, since it was previously overlooked and has lead a major change in the NFIRAOS optical design.

**Table 1:** *Flowdown of top-level requirements for the TMT early light AO system*

| Top-level requirement | Derived requirements and/or design choices |
|---|---|
| High throughput in the J, H, and K, and (as a goal) I spectral bands, with low thermal emission | • Minimize optical surface count<br>• Cooled (-30C) optical system |
| Diffraction-limited near IR image quality over a "narrow" field-of-view of 10-30 arc seconds | • Order 60x60 wavefront compensation<br>• Multi-conjugate AO (MCAO); 6 guide stars and 2 DMs |
| 50% sky coverage at the galactic pole | • Laser guide star (LGS) higher-order wavefront sensing<br>• Tip/tilt/focus natural guide star (NGS) wavefront sensing in the near infra-red over a 2 arc min diameter patrol field |
| Excellent photometric and astrometric accuracy | Stable and well characterized point spread functions:<br>• Telemetry for PSF reconstruction<br>• 3 tip/tilt and tip/tilt/focus NGS WFS to stabilize plate scale<br>*Negligible time varying image distortion at the final focal plane* |
| High observing efficiency, with a minimum of downtime and night-time calibration | Automated, reliable system |
| Available at TMT first light with low risk and affordable cost | Utilize existing and near-term technologies and design choices where possible |

## 2.2 Architecture overview

The early light AO configuration which conforms to these requirements consists of three systems: (i) the facility Narrow Field IR AO System (**NFIRAOS**), which is located on the TMT Nasmyth platform and relays light from the telescope to three science instrument ports; (ii) the Laser Guide Star Facility (**LGSF**), which generates multiple LGS in the mesospheric sodium layer as required by the NFIRAOS wavefront sensors; and (iii) the Adaptive Optics Executive Software (**AOESW**), which coordinates the operations of NFIRAOS and the LGSF with the remainder of the observatory. The locations of NFIRAOS and the LGSF are illustrated in Figure 1 below. Tables 2 and 3 summarize the technology- and subsystem design features associated with this configuration. New choices made in the last two years are *italicized* and described further below.
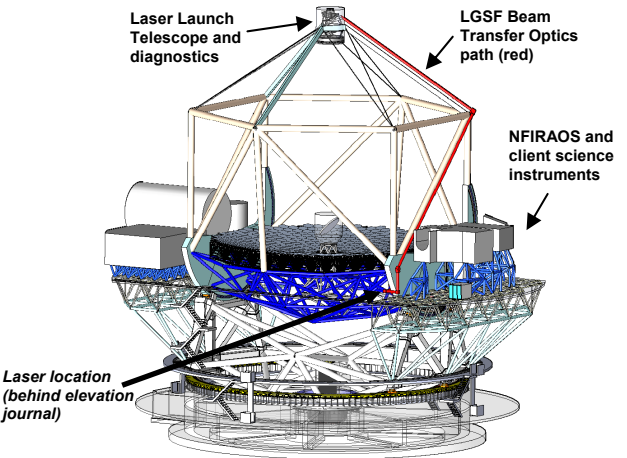


**Figure 1:** *Early light TMT AO architecture*

Table 2 lists some of the high-level design choices selected for the LGSF and NFIRAOS. The decision to project the lasers from behind the TMT secondary has been retained after a trade study against the alternative "side launch" design and a comparison of the cost, performance, and complexity of the two approaches. However, we have decided to relocate the laser systems from the azimuth structure to the elevation journal (see Figure 1). This change, made possible by the recent demonstration of smaller, lighter lasers able to operate in a variable orientation, serves to simplify and shorten the beam transfer optical path to the launch telescope. These two trade studies are described further in Section 3.1 below.

The architecture of the AO system NFIRAOS has also been re-evaluated, following the realization that the amount of field distortion present in the original optical design was incompatible with image de-rotation following NFIRAOS (at the science instrument input focus). This combination results in a time-varying distortion pattern at the instrument focal plane, which is incompatible with both high-precision astrometry and multi-object spectroscopy. The options considered to eliminate this defect were to (i) stabilize the distortion by performing the image de-rotation ahead of NFIRAOS, or (ii) modify the NFIRAOS optical design to reduce the distortion to a negligible amount. Option (ii) has been selected, following the results of the trade study discussed in Section 3.2 below. This approach leaves the location of the image de-rotator unchanged, and preserves the other NFIRAOS design features listed in Table 2.

Lastly, Table 3 updates our choices made for the critical component technologies selected for the early light AO systems. New test results over the last two years have reduced risks for all of these elements, with the sole exception of the conventional (mirror-based) beam transfer optics. Some of this progress has confirmed and developed our earlier selections (for wavefront correctors, LGS WFS detectors, and real time controller electronics), while other results provide new design options (guidestar laser systems and IR WFS detectors). Further details for each of these technologies are provided in Section 4 below.

**Table 2:** *High-Level Architecture Decisions*

| Design Choice | Decision |
| --- | --- |
| Laser launch location | Behind the TMT secondary mirror *(based upon new trade study)* |
| Laser location | *Mounted to the elevation journal on the telescope elevation structure* |
| Low-order NGS WFS location | Within each client instrument |
| Field de-rotation | At NFIRAOS-to-instrument interface *(based upon new trade study—Implies a new NFIRAOS optical design with negligible field distortion)* |
| Tip/tilt control architecture | "Woofer-tweeter" control, with a DM mounted on a tip/tilt platform |

**Table 3:** *Technologies Selected for Critical AO Components.*

| Component | Technology |
| --- | --- |
| Sodium guide star lasers | Continuous wave (CW) sum frequency *or Raman fiber laser* |
| Laser beam transport | Conventional optics (not fibers) |
| Wavefront correctors | Piezostack actuator deformable mirrors and tip/tilt stage |
| Low order, IR NGS WFS detectors | *HgCdTe CMOS array* |
| LGS WFS detectors | "Polar coordinate" CCD array |
| Real time controller (RTC) | DSP and FPGA hardware and efficient algorithms |

## 3. TRADE STUDIES AND DESIGN PROGRESS

### 3.1 Laser Guide Star Facility (LGSF)

Our original concept for the TMT LGSF was developed around two basic assumptions:

- High power guide star lasers will be large, massive, and require a fixed gravity vector;

- The noise penalties of LGS elongation are minimized by projecting lasers from behind the secondary mirror (the "center launch" configuration), just as for current AO systems on 8-10 meter telescopes with a single LGS.

These positions were challenged last year because of new demonstrations[13] and simulation results[31]. We consequently reconsidered our approach to the LGSF without these preconceptions. First, the center-launch LGSF layout was updated for a smaller, lighter laser that can operate with a variable gravity vector. Secondly, we compared this approach against possible "side launch" LGSF layouts, with lasers projected from multiple locations around the edge of the TMT primary.

The outcome of this study was to retain the center launch option, but to move the lasers from the azimuth structure to the elevation journal. The basis for this decision included a full range of performance, cost, complexity, and interface issues as outlined below.

*Side-launch laser locations:* Figure 2 illustrates the four center- and side-launch configurations considered. There are twelve locations at the edge of the primary support structure with sufficient space to mount a guide star laser with a 0.4m (refractive) launch telescope. In four locations, the assembly can be extended through the back of the support structure, providing the room to mount up to three lasers and a launch telescope. Pairing one laser per telescope requires 6 launch telescopes at first light to project the NFIRAOS asterism. Projecting 2 lasers per telescope would require at least 3 telescopes, with 4 providing a better match to the NFIRAOS asterism. We refer to these options as SL6, SL3i, and SL4i, respectively.
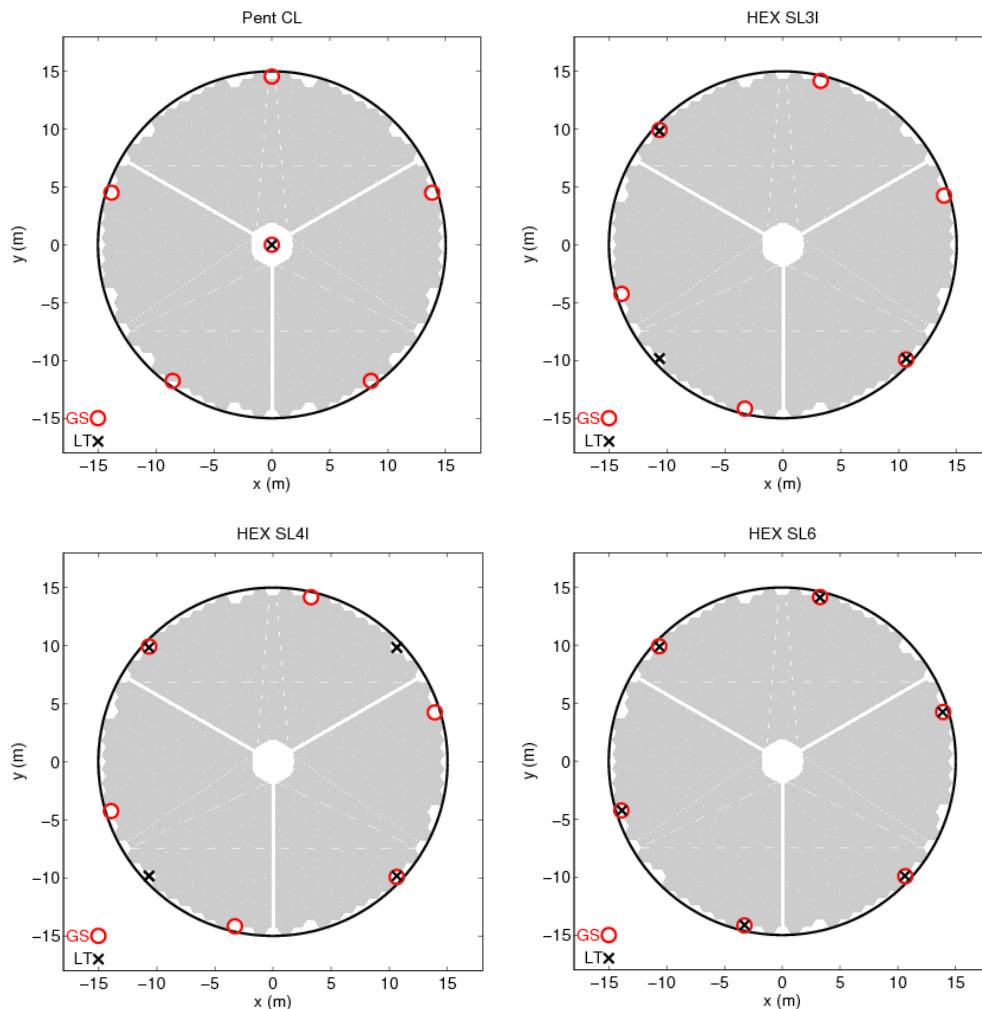


**Figure 2:** *Laser launch locations for the Center Launch (CL) and Side Launch (SL) design options. The black x's denote launch telescope coordinates in the plane of the TMT primary, and the red o's represent the locations of the laser guide stars in the sodium layer. 6, 1, and 2 lasers are projected per telescope in the CL, SL6, and SL3i options. 1 or 2 lasers are projected from each telescope for SL4i.*

*Performance Analysis:* The wavefront error due to LGS WFS measurement noise will be different for each of the laser launch options, because of the differences in the apparent elongation of the guidestar images for the case of a continuous wave laser. The amount and direction of the elongation in each WFS subaperture is proportional to the separation

between that subaperture and launch telescope coordinates in Figure 2. The maximum value of the elongation is twice as large for the side-launch configurations than for center launch, but the elongation vectors in each subaperture will be different for each guidestar due to the different launch telescope locations. These effects are compensating, and they largely cancel out according to our simulations. The performance of both approaches was comparable.

Figure 3 plots the overall higher-order wavefront error as a function of LGS WFS signal level for the four possible launch configurations. The results are based upon simulations which include physical optics models for the LGS WFSs, and also account for sodium layer thickness, the geometry of the LGS WFS polar coordinate CCD, the LGS asterism used for each launch configuration, and the NFIRAOS algorithms for WFS pixel processing and wavefront reconstruction. The performance of each option is very similar for LGS signal levels in the expected range between 900 and 450 photo-detection events per subaperture at 800 Hz, with differences of no more than 20 nm RMS.
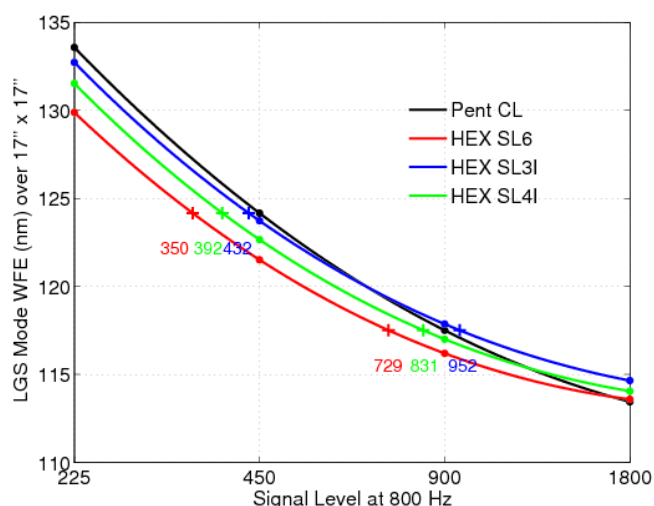
Note that the side launch option does eliminate the wavefront error due to Rayleigh backscatter crosstalk (or "fratricide") between multiple LGS WFSs. This error no more than 5-10 nm RMS for Zenith angles up to 30 degrees according to new analysis[18].

*Laser Location and Beam Transfer Optics Path:* The side-launch approach permits each laser to be placed next to its associated launch telescope, minimizing the complexity of the "beam transfer optics" between the two subsystems. Comparatively few optical elements are needed for beam steering, shuttering, sampling, and maintaining polarization. The space available to mount the launch telescopes and lasers within the primary mirror structure is quite constrained, however.
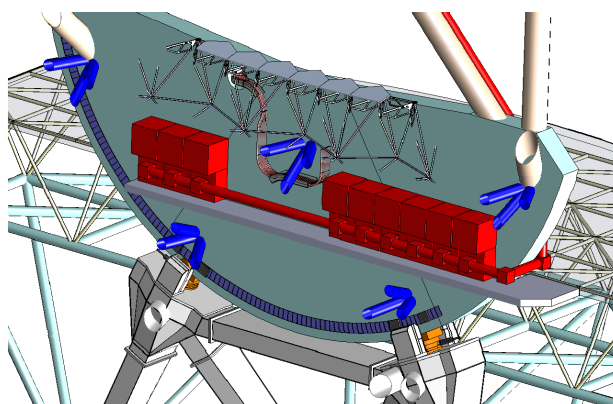
The length of the transfer optics path is much longer for the center-launch option, and the number of beam control functions is increased. Placing the lasers on the telescope top end is not presently feasible, and neither is an optical fiber beam transport system due to path lengths and power levels involved. The next best approach to simplifying the beam transfer optics is to place the lasers in the lower portion of the elevation structure, for example on the side of the elevation journal as shown in Figure 4. This requires a relatively small laser which is able to operate with a variable gravity vector.

Figure 5 is a schematic block diagram of center-launch implementation of the LGSF. As opposed to the side-launch option, the beam transfer optical path includes more optical surfaces, some of which are actively controlled to compensate for telescope flexure based upon feedback from alignment sensors at the telescope top end.



**Figure 3:** *Overall higher-order wavefront error vs. LGS WFS signal level for the four laser launch configurations. The error corresponds to the 3rd line of the error budget in Table 7 with implementation error terms neglected.*



**Figure 4:** *Updated laser location on the elevation journal*

*NFIRAOS WFS Complexity:* Due to greater LGS elongation, the number of pixels in the WFS CCD would be increased by about 40 per cent for the side launch design. The pixel processing bandwidth in the RTC is increased proportionately. Also, the asymmetrical elongation pattern rotates in the WFS pupil plane as the elevation angle changes, and must be de-rotated to remain aligned with the pixels on the polar coordinate CCD. These changes are nontrivial but not infeasible.

*Cost:* There is a moderate cost increase associated with the side launch option, based upon the range of quotes obtained for launch telescopes, beam transfer optics, and WFS modifications. The increase is too large to be justified by the small gain in performance shown in Figure 3.

*Summary:* Both the center and side launch configurations offer viable approaches for the LGSF. We have selected the former approach for TMT, due largely to comparative costs and the progress already made on designs for the TMT M1 support structure, the beam transfer optics, and the Polar Coordinate CCD array.
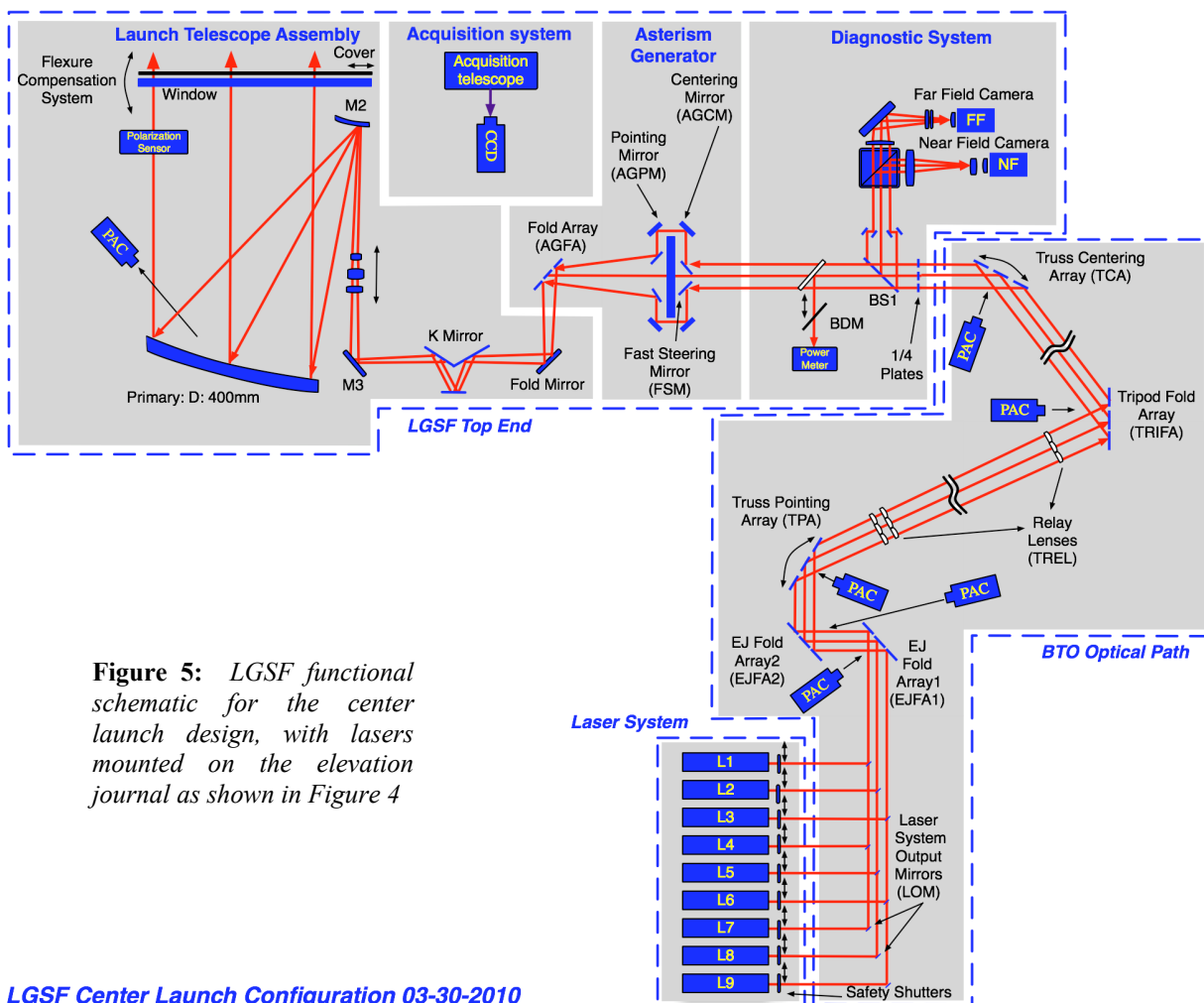


**Figure 5:** *LGSF functional schematic for the center launch design, with lasers mounted on the elevation journal as shown in Figure 4*

## 3.2 Narrow Field Infra Red AO System (NFIRAOS)

The original design of NFIRAOS was based upon the classical off-axis parabola (OAP) optical relay used in various existing AO systems. This approach was thought to be well matched to the requirements in Table 1, since it provides good image quality over the full field-of-view, minimizes the number of optical surfaces, and satisfies the packaging constraints on the TMT Nasmyth platform. However, the image plane distortion for this design is quite large (about 0.7 per cent at the edge of the 2 arcmin FoV), and the significance of this flaw was at first overlooked. Because field derotation will be implemented between NFIRAOS and its instruments, the reimaged distortion pattern will rotate with time at the science focal plane. The resulting image motion makes both multi-object spectroscopy and precision astrometry very difficult or possibly impossible for long exposure times.

A wide variety of design options have been studied to either freeze or effectively eliminate the distortion pattern. Freezing the distortion is possible if there is no motion between NFIRAOS and its instruments, which requires that field derotation be implemented ahead of NFIRAOS. Both three- and two-mirror de-rotator designs were considered; the three-element "K mirror" was rejected because the path length it consumed moved NFIRAOS off the edge of the TMT Nasmyth platform. The overall envelope of NFIRAOS with the two-element "Porro rotator" (see Figure 6) was feasible, but the de-rotator's location significantly complicated deployment of the calibration systems and sources at the input focal plane. Requirements on alignment repeatability and mirror figure could be quite challenging for a de-rotator of this size, since the distortion pattern would need to be stabilized to better than one per cent.
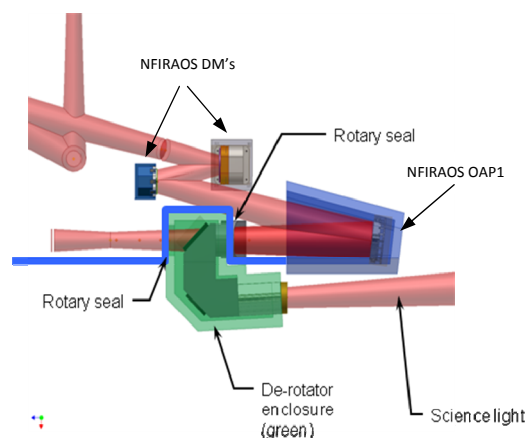
Effectively eliminating the distortion is also feasible, but requires significant changes to the dual-OAP optical design. Three different design approaches were considered:

*Aspheric corrector plates:* Although understood to be a long shot, an effort was made to cancel the distortion via aspheric correction terms on the NFIRAOS input and output windows. This approach was only able correct a modest fraction of the distortion before introducing large wavefront aberrations, specifically chromatic aberration.



**Figure 6:** *Porro rotator concept for implementing image derotation at the input to NFIRAOS. Note that in this concept, the telescope M3 mirror is adjusted to follow the moving location of the NFIRAOS input window.*
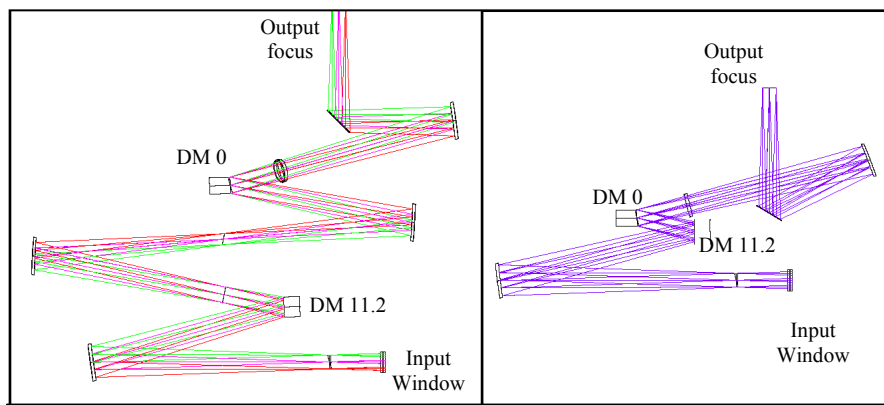
*Three- and four-mirror anastigmat designs*: Several novel optical designs were developed that were free of distortion, preserved good image quality, and added no net surfaces to the science optical path. However, these solutions required convex DMs with several millimeters of sag, as well as a concave hyperboloidal mirror much larger than the OAPs currently used in NFIRAOS. This approach was consequently rejected on the basis of cost and risk.

*Four-OAP designs:* Finally, the field distortion characteristic of the 1-to-1 OAP relay can be eliminated by placing a second relay in series with the first. There is, in fact, a solution space of allowable four-OAP designs, since the OAP focal lengths need not be identical for good performance. The optical layout and performance of our preferred solution are given in Figure 7 and Table 4. The design fits within the allow space on the TMT Nasmyth platform and meets the requirements for image quality and distortion. The four-OAP design does shift the exit pupil



**Figure 7:** *Original, dual OAP optical design for NFIRAOS (right) and the revised, four OAP design (left), on a common scale.* `

and also tightens the radius of curvature of the output focal plane, but the implications of these changes for the science instruments are acceptable.

In summary, the four-OAP design is the preferred solution for the NFIRAOS distortion problem. The strongest arguments against this approach are the large size of the opto-mechanical layout and the addition of two surfaces to the science optical path, but these consequences can be accepted given the essential requirement for correcting the distortion. Several additional benefits are now apparent after the four-OAP design has been developed, including (i) smaller non-common path aberrations in the LGS WFS optical path, and (ii) simpler implementation of the turbulence

generator and guide star source simulator optics.  These design features, and other improvements to the NFIRAOS opto-mechanical design, are described in a separate paper[12].

# 4.   AO COMPONENT DEVELOPMENT

Table 5 lists the fundamental AO performance requirements for component to be integrated into NFIRAOS and the LGSF. Progress in developing these technologies is continuing, with six new demonstrations and design studies completed or initiated over the last two years.  The most important of these results are summarized below.

## 4.1  Wavefront Correctors

NFIRAOS includes two high-order deformable mirrors (DMs) to implement dual conjugate, order 60x60 wavefront correction on a thirty meter aperture.  The large aperture implies the need for 10 μm actuator stroke, and low hysteresis is required for maximum control bandwidth.  The mirrors must also operate at the -30C temperature of the NFIRAOS optical path. These actuator performance requirements were demonstrated by the subscale 9x9 prototype DM fabricated and tested by CILAS in 2006, as presented previously[25].  More recently, a 41x41 CILAS DM has been successfully delivered for the ESO SPHERE system, using the same materials and components in a very similar design[25].

NFIRAOS will also include a tip/tilt stage (TTS) to stabilize the overall line-of-sight, since controlling this mode would require unacceptable stroke from the DM actuators.  The TTS acts as the mount for the ground-conjugate DM, so that the tip/tilt correction is applied at a pupil and does not induce beam motion at wavefront sensors or instrument cold stops.  This approach avoids the additional optical surface(s) introduced by a separate tip/tilt mirror, but the requirements for the TTS are very different from what has been demonstrated in other systems.  In particular, the mass (32 kg), clear aperture (30 cm) actuator count (2.7K) of the DM for NFIRAOS are all much larger than for any other DM mounted in a TTS to date.
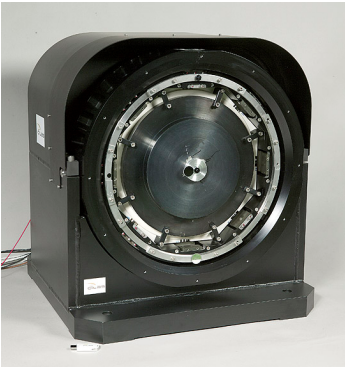
**Table 5:** *Top-level  requirements for AO components*

| Component | Key Requirements |
|---|---|
| Deformable mirrors | 63x63 and 76x76 actuators at 5 mm spacing<br>10 μm stroke and 5% hysteresis at -30C |
| Tip/tilt stage | 500 mrad stroke with 0.05 mrad noise<br>20 Hz bandwidth |
| NGS WFS detector | 240x240 pixels<br>~0.8 quantum efficiency,~1 electron at 10-800 Hz |
| LGS WFS detectors | 60x60 subapertures with 6x6 to 6x15 pixels each<br>~0.9 quantum efficiency, 3 electrons at 800 Hz |
| Low-order IR NGS WFS detectors | 1024x1024 pixels (subarray readout on ~8x8 windows)<br>~0.8 quantum efficiency, 3 electrons at 10-200 Hz |
| Real time controller | Solve 35k x 7k reconstruction problem at 800 Hz |
| Sodium guidestar lasers | 25W, near diffraction-limited beam quality<br>Coupling efficiency of 130 photons-m$^2$/s/W/atom |



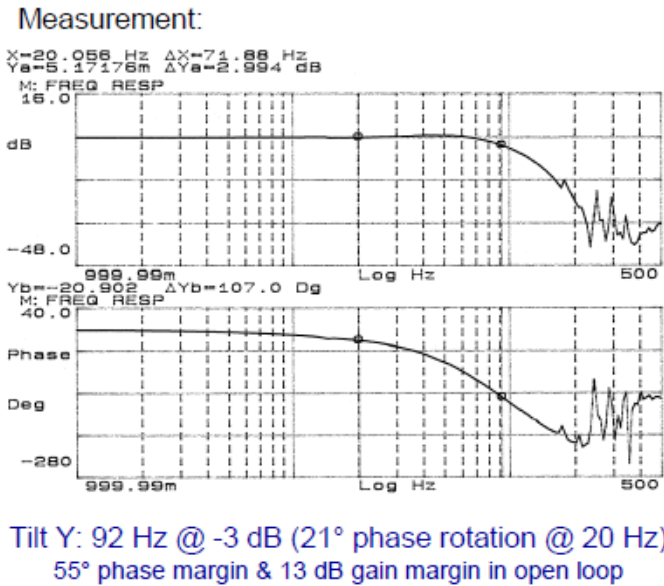**Figure 8:**  *Full-size CILAS tip/tilt stage prototype*



**Figure  9:**  *CILAS prototype tip/tilt stage bandwidth measurement*

CILAS has now fabricated and tested a full-scale prototype of the TTS. All requirements for stroke, precision, and bandwidth have been demonstrated with a dummy payload simulating the NFIRAOS DM and its wiring, both at room temperature and at -30C. The 20 Hz bandwidth requirement has been surpassed, with results from 90 to 100 Hz demonstrated.
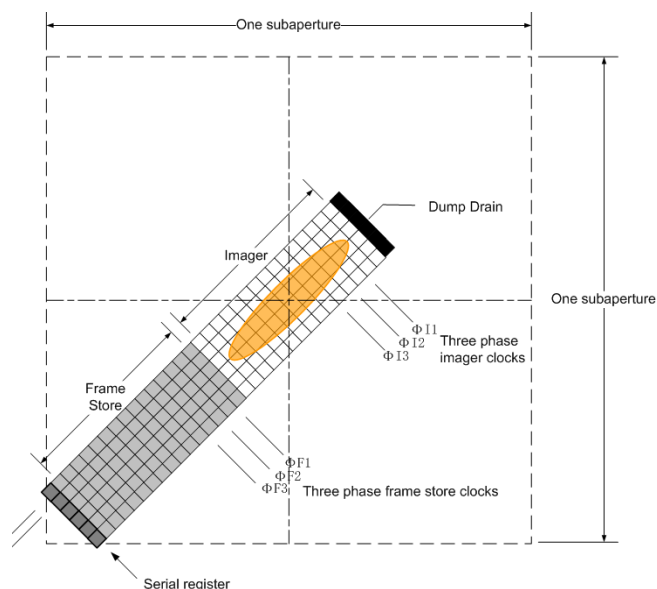
Figures 8 is a photograph of the TTS prototype, and sample test results are plotted in Figure 9. The TTS is now at HIA, where it will undergo additional characterization. It will then be returned to CILAS, where the electronics, control software, and mechanical interfaces will be upgraded to the final specifications for NFIRAOS.

### 4.2 Visible Wavefront Sensing Detectors

NFIRAOS incorporates 6 LGS and 1 NGS Shack-Hartmann WFSs with 60x60 subapertures. A pair of designs for low-noise, high-speed CCDs have been developed by W.M. Keck Observatory and MIT Lincoln Laboratory, with funding provided by the NSF Adaptive Optics Development Program (AODP). Prototypes of both detectors are now being fabricated in a wafer run supported by TMT, W.M. Keck Observatory, and the USAF Starfire Optical Range. Initial test results for these prototypes will be available in late 2010.

The NFIRAOS strategies for LGS wavefront sensing and processing are defined to minimize the measurement errors due to the depth and variability of the mesospheric sodium layer. The LGS WFS cameras will employ a "polar coordinate" CCD, with a small, separate subarray of pixels for each WFS subaperture. The size and orientation of each subarray is matched to the LGS spot elongation, which is proportional to the separation between the locations of launch telescope and WFS subaperture projected onto the TMT primary. This design will (i) minimize number of pixels, and therefore also pixel read rate and read noise; (ii) simplify the implementation of noise-optimal pixel processing algorithms, and (iii) enable dynamic refocusing (via properly timed charge shifting) to eliminate LGS spot elongation for lasers with pulse lengths of several µsec, if and when such lasers become available.

The CCD array design for the NGS WFS camera is more conventional, since the guidestar images in each subaperture are roughly symmetric, seeing-limited spots.



a. *Illustration of one subaperture, with an elongated LGS spot imaged on 6x15 pixels*
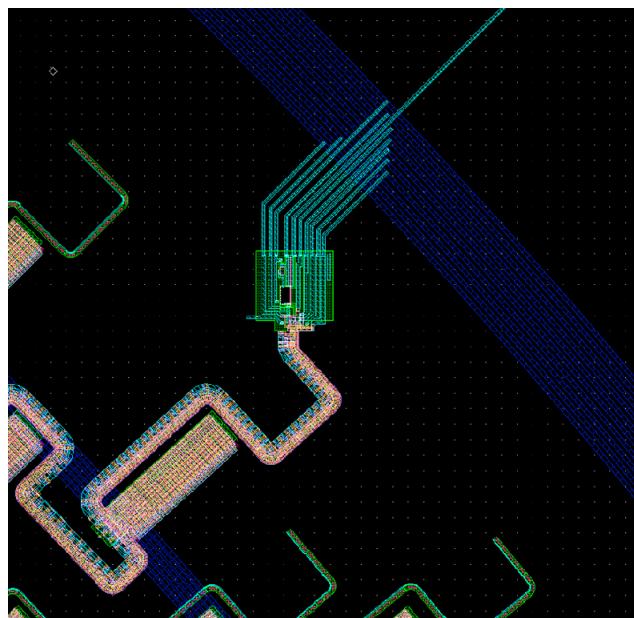


b. *Subsection of the prototype mask design illustrating one edge subaperture a serial register, and an output amplifier*

**Figure 10:** *Polar coordinate CCD concept and prototype design*

A square CCD of 256x256 pixels will be used, to provide 4x4 pixels for each of the 60x60 subapertures. Both CCDs will utilize a 2-stage planar JFET amplifier, which has already been demonstrated in a 160x160 CCD during the first phase of the AODP project. Based on these results, the polar coordinate CCD is expected to achieve 3 read noise electrons at a full frame readout time of 500 µsec. The NGS CCD is expected to achieve one electron read noise for frame times from 5 to 20 msec, because of the much lower pixel read rate.

The ongoing wafer run will fabricate a one-quadrant section of the polar coordinate CCD. The full scale design is a four-fold replication of this single quadrant. The 256x256 CCD is a full scale prototype of the NGS WFS detector, and it could be used in NFIRAOS if performance is acceptable.

### 4.3 Infra-Red Wavefront Sensing Detectors

Low order (2x2 subaperture) NGS WFSs will be required in each NFIRAOS client instrument, since laser guide stars cannot (currently) measure global tip/tilt, and are also subject to drift in focus measurements as the altitude of the sodium layer varies. For optimal image quality, three sensors will be needed to measure tilt anisoplanatism in addition to overall tip/tilt. Tip/tilt sensing in the infra-red (J and H bands) instead of the visible (R and I) can potentially improve sky coverage due to the higher frequency of K and M class stars, and also because of the NGS image "sharpening" provided by NFIRAOS at IR wavelengths. However, these advantages can only be achieved given the availability of high speed, low-noise, large format IR detectors with flexible readout modes.

A detector with roughly 1024 x 1024 pixels is preferred for this application, given dual requirements for a large field of view (~4 arc sec) for initial acquisition and the simultaneous need for Nyquist rate image sampling in J and H band (~4 mas) to provide linear WFS measurement with uniform gain. Once the tip/tilt loop is closed, however, the necessary guide window is about 4x4 or 6x6 pixels per subaperture. Requirements derived from sky coverage simulations (see section 5) include quantum efficiency of 0.8 and read noise of about 3 electrons at frame rates of 80 to 100 Hz, Finally, the readout electronics must be sufficiently flexible to shrink the readout window as acquisition converges, and translate it across the detector during on-chip dithering.

The Teledyne H2RG HgCdTe detector provides a first approximation to these requirements. Tests at Caltech using correlated multiple sampling have achieved ~3 electrons read noise at the required pixel read rate on small guide windows. We intend to monitor new developments that would reduce costs or improve performance, but the H2RG array provides one acceptable solution for low order IR wavefront sensing for TMT.

### 4.4 Real Time Controller (RTC) Algorithms and Processing Algorithms

The RTC is one of the more challenging AO subsystems. Its requirements include real time pixel processing for the high-order LGS and low-order NGS WFSs, tomographic wavefront reconstruction, calculation of DM actuator commands, and real-time optimization of the algorithms for these processes as conditions change. It also acquires DM and WFS telemetry in order to reconstruct (i.e., estimate) the science PSF for image post-processing. The RTC interfaces with the wavefront sensing- and correcting components within NFIRAOS, at I/O and computation rates which are several orders of magnitude more demanding than found in today's astronomical AO systems. Significant progress in developing designs that meet these requirements has been made over the last two years.

Two RTC conceptual design studies were conducted for TMT from mid-2008 through mid-2009. One study was performed by the Optical Sciences Company with support from Montana State University. The second study was lead by Dominion Radio Astrophysics Observatory and also included Lyrtech and the University of Victoria. Both groups developed successful designs meeting all performance requirements, and in some cases many goals, for the NFIRAOS RTC. Both studies implemented the processing algorithms specified by TMT in designs based upon existing field programmable gate arrays (FPGAs) and digital signal processors (DSPs), in electronics packages meeting the requirements for rack space, mass, and power dissipation. After these studies, the development of the NFIRAOS RTC is now sufficiently advanced to proceed to a Preliminary Design Phase at the beginning of the TMT construction phase.

### 4.5 Guide Star Laser Systems

Recent progress for this component has also been highly encouraging. Table 6 summarizes the revised top-level requirements for the first light TMT laser systems. The performance requirements are generally consistent with earlier versions, but many functional requirements have been changed due to the new LGSF layout described in Section 3.1.

The new requirements represent a significant advance over existing guide star laser currently deployed, but their feasibility has been demonstrated during 2009 in two Preliminary Design Studies performed by FASORtronics and TOPTICA for the European Southern Observatory (with additional support for risk reduction provided by AURA). The new lasers are designed to be aligned remotely, with preventative maintenance performed by exchanging enclosed modules. These features enable the placement of the lasers along the inside face of the TMT elevation journal, as illustrated in Figure 4.

ESO is now proceeding to the Final Design Phase for one of these designs, towards the eventual procurement of four lasers for the new Laser Guide Star Facility at the Very Large Telescope (VLT). Keck Observatory and TMT have submitted an NSF proposal to procure one laser (from the same vendor) for Keck II, with a future plan for two additional lasers for the Keck Next Generation AO (KNGAO) system. This development path will help to retire most remaining risks for the TMT lasers, which are to be procured approximately one year following the start of our construction phase.

**Table 6:** *Top-level laser system requirements*

| Laser parameter | Requirement |
|---|---|
| Pulse format | CW or quasi CW |
| Average power, W | 25 |
| Far field beam quality | 95% of energy contained in a Gaussian mode no broader than 1.05 times diffraction limited |
| Sodium coupling efficiency, photons-m$^2$/s/W/ion | 130 |
| Mass, kg | Laser head < 500<br>Laser electronics < 250 |
| Dimensions, m | Laser head < 1.0 x 0.6 x 1.0<br>Laser electronics < 1.0 x 1.0 x 1.0 |
| Operating gravity orientation | 0 to 65 degrees |

## 5. AO MODELING AND PERFORMANCE ANALYSIS

The principal image quality requirement for early light AO is an on-axis RMS wavefront error (WFE) of 187 nm at the instrument focal plane. This must be achieved for median turbulence conditions with 50 per cent sky coverage at the galactic pole. Table 7 outlines our estimated performance, which meets requirements with contingency of 86 nm RMS.

This table represents the outcome of considerable new work over the past two years, even though the overall result is similar to previous performance estimates[29]. New simulations have been performed for Mauna Kea turbulence profiles, and the wavefront maps used for representative telescope aberrations have also been updated. The parameters for AO hardware components have been revised as necessary, including the values used for DM actuator influence functions, tip/tilt stage bandwidth, and optical throughput, quantum efficiency, and read noise for the NGS and LGS WFS channels. The modeling of the low-order (tip/tilt and tip/tilt/focus) NGS sensors now simulates the partially "sharpened" guide star images using physical optics, and new sky coverage estimates are based upon Monte Carlo simulations of 500 guide star fields. The simulation code used for WFS pixel processing and wavefront reconstruction has been updated to match the algorithms planned for the actual RTC. This includes the overall "split tomography" control architecture, the conjugate gradient (CG) or Cholesky backsolve (CBS) methods for efficient wavefront reconstruction of LGS WFS measurements, the matched filter pixel processing algorithms for both the LGS and NGS WFSs, and optimized type II "woofer-tweeter" servo filters for the NGS control loops.

Finally, the errors due to additional implementation effects have now been quantified through a mix of simulation upgrades, independent analyses, and/or new lab and field tests. These terms include the LGS WFS "fratricide" effect due to Rayleigh backscatter, LGS WFS defocus and higher-order measurement errors due to unknown variations in the sodium layer, and sub-optimality of the wavefront reconstruction due to imperfect knowledge of the turbulence profile. See the companion papers on AO simulations for details[16-19,22].

## 6. LAB AND FIELD TESTS

Two research projects are now underway to validate aspects of the NFIRAOS control architecture and to measure the temporal and spatial variability of the mesospheric sodium layer. The University of Victoria Laser Guide Star Wavefront Sensor Test Bench[20,27] has implemented the full set of real-time algorithms and background processes planned for the LGS wavefront sensing architecture, including: Wavefront gradient measurement via matched filtering, real-time updating

**Table 7:** *Summary AO error performance estimate*

| Error term | On-axis RMS WFE, nm |
|---|---|
| Total error | 187 |
| LGS mode error | 154 |
| First-order turbulence compensation | 122 |
| Implementation errors | 95 |
| Opto-mechanical | 74 |
| AO component and higher-order effects | 59 |
| NGS mode error | 62 |
| Contingency | 86 |

of the filter gains to adapt to sodium layer variations, and real-time updating of the matched filter offsets using a low-bandwidth NGS "truth" (or calibration) wavefront sensor. The performance of the overall system is stable, and can be predicted and optimized using knowledge of the transfer functions of the individual sensors and control laws. Further experiments will assess the long-term performance of the full set of LGS WFS processing algorithms for measured histories of the sodium layer.
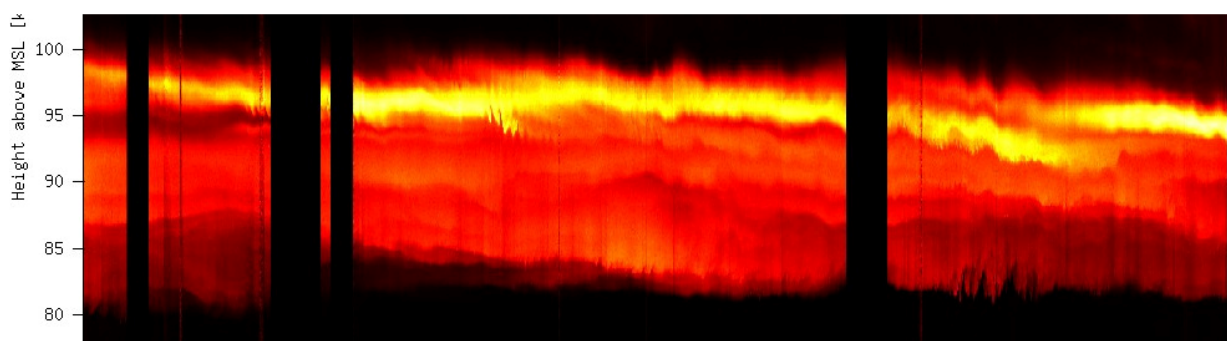
These sodium layer measurements have been recorded with the University of British Columbia LIDAR system[21], which employs a pulsed 5W dye laser and a 6m receiver to observe the mesospheric sodium layer with a range resolution of about 5m at 50 Hz (see Fig. 11). The system has confirmed that the power spectrum of the mean range to the layer follows a $f^{-1.9}$ power law to a frequency of at least 10 Hz. The bandwidth of these results extends 1-2 orders of magnitude beyond previous measurements (Fig. 12) and the power law has been used to determine the NFIRAOS error due to LGS focus uncertainty. This LIDAR system also enables the study of "sporadic" micro-meteorite events at resolutions which were previously impossible. Observations are continuing this summer with a new, higher-speed photon counter and a fast steering mirror to simulate multi-guidestar asterisms.

## 7. SUMMARY

The overall architecture of the TMT first light adaptive optics has seen significant revisions during the last year to eliminate an oversight regarding image distortion in the original design of NFIRAOS, and to adapt the layout of the LGSF to exploit the recent improvements to guide star laser systems. The last two years have also seen important advances in the development and demonstration of the AO hardware components for TMT, including wavefront correctors, LGS and NGS wavefront sensing detectors, RTC control algorithms and processors, and guidestar laser systems. The predicted performance of the system remains stable as higher fidelity models are implemented and simulation parameters are updated based upon new lab- and field test results. The overall AO effort will be ready for the TMT Construction Phase once the design of the revised NFIRAOS reaches the Preliminary Design level.

## ACKNOWLEDGEMENTS

**Figure 11:** *High resolution sodium layer time history measured using the University of British Columbia LIDAR system*
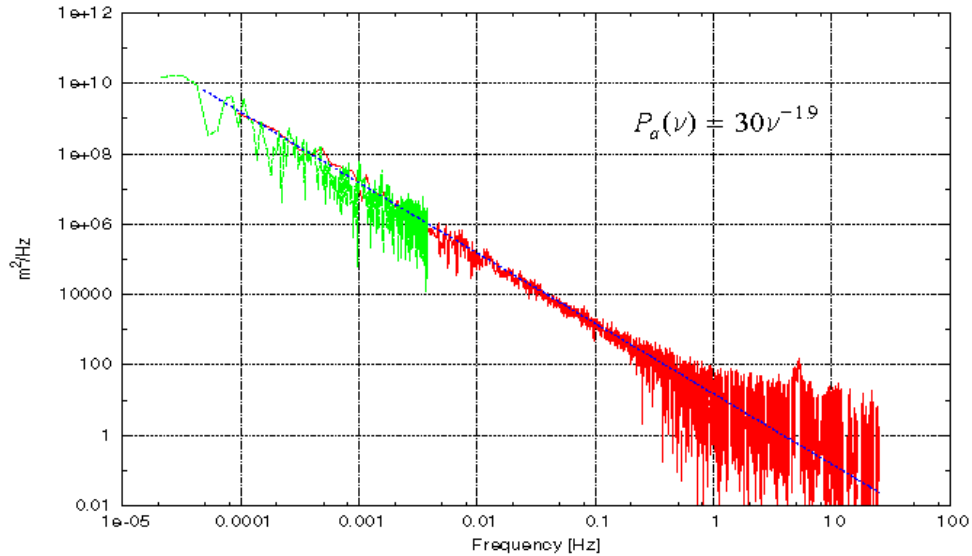
**Figure 12:** *Previous (green) and new UBC (red) power spectra measurements of the mean range of the sodium layer*

# REFERENCES

[1] G. Sanders and J. Nelson, "The status of the Thirty Meter Telescope project", Proc. SPIE 7733-69 (2010).

[2] G. Z. Angeli, S. Roberts, and K. Vogiatzis, "System Engineering for the Thirty Meter Telescope," Proc. SPIE 7738-45 (2010).

[3] M. Troy, G. Chanan, P. Dumont, and J. Roberts, "Shack-Hartmann Phasing of Segmented Telescopes Using Fresnel Diffraction," Proc. SPIE 7733-81 (2010).

[4] M. W. Regehr, P. M. Thompson, and M. M. Colavita, "Dynamic Characterization of a Prototype of the Thirty Meter Telescope Primary Segment Assembly, Proc. SPIE 7733-85 (2010).

[5] D. G. MacMynowski, P. M. Thompson, C. Shelton, and L. C. Roberts, Jr., "Robustness of Thirty Meter Telescope Primary Mirror Control, Proc. SPIE 7733-189 (2010).

[6] L. Simard, C. Boyer, D. Crampton, and B. Ellerbroek, "The TMT Instrumentation Program," Proc. SPIE 7735-73 (2010).

[7] L. Simard and D. Crampton, "Science Flowdown for the Thirty Meter Telescope," Proc. SPIE 7735-213 (2010).

[8] J. E. Larkin, A. F. Moore, E. J. Barton, B. Bauman, K. Bui, J. Canfield, D. Crampton, A. Delacroix, M. Fletcher, D. Hale, D. Loop, C. Niehaus, A. C. Phillips, V. Reshetov, L. Simard, R. Smith, R. Suzuki, T. Usuda, and S. A. Wright, "The Infrared Imaging Spectrograph (IRIS) for TMT: Instrument Overview," Proc. SPIE 7735-79 (2010).

[9] B. Mobasher, R. W. Weber, N. Konidaris, D. Crampton, L. Simard, "An Infra-Red Multi-object Spectrograph (IRMS) with Adaptive Optics on the TMT: Overview and Science Case," Proc. SPIE 7735-211 (2010).

[10] M. Schoeck, S. G. Els, R. L. Riddle, W. A. Skidmore, and T. Travouillon, "Open questions in site characterization and turbulence parameter measurements," Proc. SPIE 7736-70 (2010).

[11] TMT Detailed Science Case, http://www.tmt.org/foundation-docs/TMT-DSC-2007-R1.pdf (2007).

[12] G. Herriot, D. Andersen, J. Atwood, C. Boyer, P. Byrnes, R. Conan, B. Ellerbroek, J. T. Fitzsimmons, L. Gilles, P. Hickson, A. Hill, K. J. Jackson, O. Lardière, T. Pfrommer, J.-P. Véran, L. Wang, and Ivan Wevers, "NFIRAOS: facility adaptive optics system for the TMT," Proc. SPIE 7736-9 (2010).

[13] S. K. Adkins, "Laser systems for laser guide star adaptive optics: status and perspectives," Proc. SPIE 7736-64 (2010).

[14] D. D. S. Hale, R. M. Smith, G. Rahmer, D. Loop, B. L. Ellerbroek, and L. Wang, "NIR low-order wavefront sensor for TMT IRIS," Proc. SPIE 7736-36 (2010).

[15] R. Conan and J.-P. Veran, "Introduction to advanced real-time control algorithms," Proc. SPIE 7736-38 (2010).

[16] L. Gilles and B. Ellerbroek, "Split atmospheric tomography for multiconjugate and multi-object adaptive optics," Proc. SPIE 7736-31 (2010).

[17] L. Gilles and B. Ellerbroek, "Real-time turbulence profile estimation from closed-loop laser guide star wavefront sensor measurements," Proc SPIE 7736-143 (2010).

[18] L. Wang, A. Otarola, and B. L. Ellerbroek, "Impact of laser guide fratricide on TMT MCAO system," Proc. SPIE 7736-16 (2010)

[19] J.-P. Véran, C. Irvin, and G. Herriot, "Implementation of type-II tip-tilt control in NFIRAOS, with woofer-tweeter and vibration cancellation," Proc. SPIE 7736-167 (2010).

[20] R. Conan, J.-P. Veran, and K. J. Jackson, "Experimental validation of type-II tip-tilt control in a woofer-tweeter adaptive optics system," Proc. SPIE 7736-169 (2010).

[21] T. Pfrommer and P. Hickson, "High-resolution mesospheric sodium observations for extremely large telescopes," Proc. SPIE 7736-71 (2010).

[22] G. Herriot, R. Conan, P. Hickson, K. J. Jackson, O. Lardière, and T. Pfrommer, "Transients in the sodium layer: assessment and mitigation for TMT," Proc. SPIE 7736-178 (2010).

[23] C. Boyer, B. Ellerbroek, L. Gilles and L. Wang, "The TMT Laser Guide Star Facility," in *Adaptive Optics for Extremely Large Telescopes,* Y. Clénet, J.-M. Conan, T. Fusco and G. Rousset, Eds. (2009).

[24] G.J. Hovey, R. Conan, F. Gamache, G. Herriot, Z. Ljusic, D. Quinn, M. Smith, J.P. Veran and H. Zhang, "An FPGA Based Computing Platform for Adaptive Optics Control," in *Adaptive Optics for Extremely Large Telescopes,* Y. Clénet, J.-M. Conan, T. Fusco and G. Rousset, Eds. (2009).

[25] J.-C. Sinquin, J.-M. Lurcon, and P. Morin, "Piezo Array Deformable Mirrors and New Associated Technologies: Spherical Shape and Tip/Tilt Mount," in *Adaptive Optics: Methods, Analysis and Applications*, OSA Technical Digest (CD) (Optical Society of America, 2009), paper AOThD3.

[26] L. Wang and B. Ellerbroek, "High Fidelity Sky Coverage Analysis and Long Exposure PSF Modeling for Multi-Conjugate AO," ibid, paper AOTuD2.

[27] R. Conan, O. Lardiere, and K. Jackson, "Comparison of Self-Referenced Center of Gravity, Quad-Cell and Matched Filter Algorithms for Laser Guide Star Wavefront Sensing," ibid, paper AOTuB2.

[28] TMT Observatory Requirements Document, http://www.tmt.org/foundation-docs/ORD-CCR18.pdf (2008).

[29] B. Ellerbroek, S. Adkins, D. Andersen, J. Atwood, C. Boyer, P. Byrnes, R. Conan, L. Gilles, G. Herriot, P. Hickson, E. Hileman, D. Joyce, B. Leckie, M. Kiang, T. Pfrommer, J-C. Sinquin, J-P. Veran, L. Wang, and P. Welle, "Progress toward developing the TMT adaptive optical systems and their components," Proc. SPIE 7015 (2008).

[30] B. Ellerbroek, "Adaptive Optics Systems for the Thirty Mirror Telescope," in *Adaptive Optics for Extremely Large Telescopes,* Y. Clénet, J.-M. Conan, T. Fusco and G. Rousset, Eds. (2009).

[31] C. Robert, Jean-Marc Conan, D. Gratadour, C. Petit and T. Fusco, "Shack-Hartmann tomographic wavefront reconstruction using LGS: analysis of spot elongation and fratricide effect," in *Adaptive Optics for Extremely Large Telescopes,* Y. Clénet, J.-M. Conan, T. Fusco and G. Rousset, Eds. (2009).